Controlled Atomic Spontaneous Emission from Er^{3+} in a Transparent Si/SiO_2 Microcavity

A. M. Vredenberg, N. E. J. Hunt, E. F. Schubert, D. C. Jacobson, J. M. Poate, and G. J. Zydzik
AT&T Bell Laboratories, Murray Hill, New Jersey 07974
(Received 27 January 1993)

The spontaneous emission lifetime and intensity of Er implanted into SiO_2 is modified by a Si/SiO_2 planar microcavity. The cavity strongly affects the coupling of the optically excited Er^{3+} to the radiative and waveguiding modes of the system, resulting in a spontaneous lifetime of 14.8 ms for a cavity off-resonance with the Er^{3+} versus a lifetime of 9.1 ms for an on-resonance cavity. The observed spontaneous emission lifetime changes agree well with calculated values based on a computation method which is also presented.

PACS numbers: 42.50.−p, 32.70.Fw, 32.70.Jz, 78.66.Jg

There has been much recent attention regarding the use of planar microcavities to demonstrate fundamental changes in the spontaneous emission rates and spectra of emitting media. After cavity effects at radio frequencies were first proposed by Purcell [1] in 1946, other authors [2] have demonstrated that confocal resonators indeed can drastically modify the spontaneous emission lifetime of an atom within a resonator of millimeter wavelengths. This concept has been extended to short planar cavities at optical wavelengths, where experiments using flowing dye [3], dye-containing films [4], and semiconductors [5] as the active media have demonstrated significant lifetime changes. None of these experimental results in planar cavities, however, was quantitatively compared to theoretical models. Nonradiative energy loss processes, pump-dependent spectra, and the effects of self-absorption of emitted light by the active media [6] can affect the measured lifetimes. In our experiment, we measure the spontaneous lifetime changes of the $^4I_{13/2} \rightarrow {}^4I_{15/2}$ transition of Er^{3+} ions (emission wavelength ~ 1535 nm) implanted at low concentration into a thin (half-wavelength) SiO_2 film, surrounded by high-reflectivity Si/SiO_2 planar distributed Bragg reflectors. The Er^{3+} ions exhibit atomic, intra-$4f$, electronic transitions which are effectively shielded by the outlying $5s^2$ and $5p^6$ electrons, and the probed $^4I_{13/2} \rightarrow {}^4I_{15/2}$ transition has a nearly 100% quantum efficiency [7]. This system is thus ideal for measuring cavity-induced lifetime changes because of the small self-absorption of the Er^{3+} ions, and the narrow atomic emission spectrum. This enables us to compare, for the first time, active-media lifetimes for various thickness planar resonators with calculated values. These result from a general computation method which is also presented.

The Er-doped SiO_2 active region ($\lambda/2$) is ~ 540 nm thick and is surrounded by distributed Bragg reflectors (DBRs), which are composed [8] of 4 (bottom) and $2\frac{1}{2}$ pairs (top) of Si (115 nm) and SiO_2 (270 nm) quarter-wave layers, e-beam deposited on a Si substrate. The calculated bottom and top mirror reflectivities (R_{bot} and R_{top}) are 99.8% and 98.5%, respectively. Implantation of 800 keV, 1×10^{15} Er^+/cm^2 into the active region was performed prior to deposition of the top DBR, in order to yield a sharp concentration profile (full width at half maximum ~ 260 nm) just below the center plane of the active region. The Er concentration was below 0.2 at.%, assuring that luminescence concentration quenching was negligible [9] and that significant absorption or gain could not occur [7]. After implantation the samples were annealed in a vacuum furnace at 900 °C for 30 min in order to remove ion-induced defects and simultaneously optically activate the Er^{3+} ions [9]. On part of the sample a top DBR was then deposited, completing the cavity. The on-axis cavity resonance wavelength (λ_{res}) was determined by reflectivity measurements which exhibit a dip in the reflectivity at resonance.

A Ti:sapphire laser, operating at 980 nm, was directed at an angle $\sim 30°$ to the sample axis to optically excite the Er^{3+} ions. Figure 1 compares photoluminescence (PL) spectra of a cavity implanted through the entire top

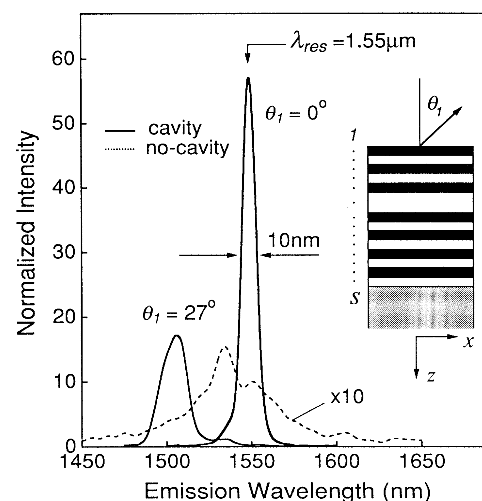

FIG. 1. The natural Er^{3+} photoluminescence spectrum, amplified by 10, from the active region of a microcavity without top mirror (dashed line), and the PL spectra of Er^{3+} from a resonant cavity at 0° and 27° from the normal. All spectra were recorded in exactly the same geometry and are normalized to the luminescence intensity of the noncavity structure at 1.55 μm (λ_{res} of the cavity).

0031-9007/93/71(4)/517(4)$06.00

© 1993 The American Physical Society

mirror, and the same structure with the top mirror etched away. The spectrum from the no-cavity structure (i.e., without top DBR) exhibits a typical [7,9] tailing double peak structure, with the strongest peak at 1535 nm. The spectra from the cavity are markedly different: The peak intensities are enhanced [8] by nearly 60, compared to the no-cavity yield at the corresponding wavelengths; the spectrum taken along the optical axis ($\theta_l = 0°$) peaks at λ_{res}, with a reduced width of ~ 10 nm, while the peak position shifts towards shorter wavelengths for higher θ_l ($\theta_l = 27°$). The intensity enhancement occurs because at any particular wavelength the emission rate into a resonant cavity mode (which is highly directional) is increased, while in almost all other directions it is reduced. This redistribution of emitted intensity is a well-known cavity effect and has been observed in a number of other cavity structures [10]. For emission on the optical axis through the top reflector, the peak emission rate enhancement factor, G, for excited ions in the resonance antinode position can be shown to be

$$G = (1 + \sqrt{R_{bot}})^2 (1 - R_{top})/(1 - \sqrt{R_{bot} R_{top}})^2 .$$

In contrast to previously published equations [8,11,12] for G, this equation is valid for all combinations of R_{bot} and R_{top} [13]. To obtain the true intensity enhancement factor, G should be multiplied by the ratio of the excited state lifetimes with and without the cavity τ_{cav}/τ_0, but this is only a minor correction (see fluorescence decay studies below). Thus, the emission rate enhancement, compared to bulk SiO_2:Er, is calculated to be $G = 825$. However, we measure the enhancement ratio between the cavity and no-cavity structure. This ratio is calculated to be 320, using a more extended computation method (see below), which also takes into account the implanted Er distribution. The difference with experiment results from our 10 nm linewidth which is wider than the theoretical 2.5 nm resonance width following from R_{bot} and R_{top}. This broadening is a result of nonideal mirror reflectivities and a finite emission collection angle, and reduces the theoretical peak intensity ratio to 80, which is close to what is observed. For wavelengths $< \lambda_{res}$, the emission spreads away from the cavity axis (see the curve for $\theta_l = 27°$ in Fig. 1), as the cavity resonance shifts toward lower wavelengths when the cavity is viewed from any angle [8,10].

The cavity is also expected to change the *total* emission rate of the excited Er^{3+} ions, which can be probed with luminescence decay measurements. Thus, for a cavity with λ_{res} larger than the average emission wavelength, the emission rate should increase, characterized by a shorter excited state lifetime, and vice versa for λ_{res} at shorter wavelengths [1]. We first demonstrate this for the latter case. Time-resolved luminescence measurements after pulsed excitation were performed by mechanically chopping the exciting laser beam and monitoring the signal on a digital LeCroy 9410 oscilloscope. In Fig. 2, the luminescence from a structure before top mirror deposition (curve *a*) showed single-exponential decay, characterized by a lifetime of 9.5 ms. Deposition of the top DBR then resulted in a 1.44 μm cavity and the luminescence decay of this structure (curve *b*) had a lifetime of 13.7 ms, indeed longer than in the no-cavity structure. Finally, the top mirror was removed through selective wet etching. The lifetime of this structure was 9.5 ms (curve *c*), comparable to the (similar) situation before the deposition of the top mirror. Since photon reabsorption effects can be excluded, the observed lifetime enhancement is indeed a real cavity effect and reflects a modified transition probability from the excited to the ground state due to a different coupling of the excited ion with light-wave modes in the cavity.

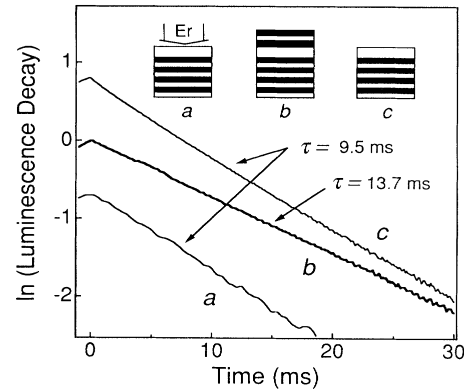

FIG. 2. PL decay curves for three stages of microcavity preparation: (a) after 800 keV Er^+ implantation into the SiO_2 active region and 900 °C anneal, (b) after deposition of the top DBR, creating a cavity resonant at 1.44 μm, and (c) after removal of the top mirror by etching. The curves are normalized to their peak intensities at $t = 0$; for clarity sake, traces *a* and *c* are up and down shifted over 0.8, respectively.

We then prepared a series of cavities with different active region thicknesses, by cutting an 800 keV, 1×10^{15} Er/cm^2 implanted and annealed structure without top DBR into an array of samples and by etching each of these to a different active region thickness using a buffered HF solution. After deposition of the top DBR on the complete cavity set, the resulting resonance wavelengths varied from 1.41 to 1.65 μm, thus spanning the entire Er^{3+} luminescence peak. The structure with the thickest active region, but without top mirror, was chosen as a reference sample. Decay measurements were performed on the cavities and the reference sample and the ratio of the cavity lifetime (τ_{cav}) to the reference lifetime ($\tau_{ref} = 10.9 \pm 0.1$ ms) was calculated for each cavity. Figure 3 shows the resulting normalized emission rates $(\tau_{cav}/\tau_{ref})^{-1}$ versus λ_{res}. The measurements clearly follow the trend which was anticipated above. For $\lambda_{res} \lesssim 1535$ nm, the emission rate is decreased compared to the reference structure (with a corresponding maximum τ_{cav} of 14.8 ms), because more than half of the emission is suppressed. For $\lambda_{res} \gtrsim 1535$ nm, the emission rate is increased over that of the reference value and

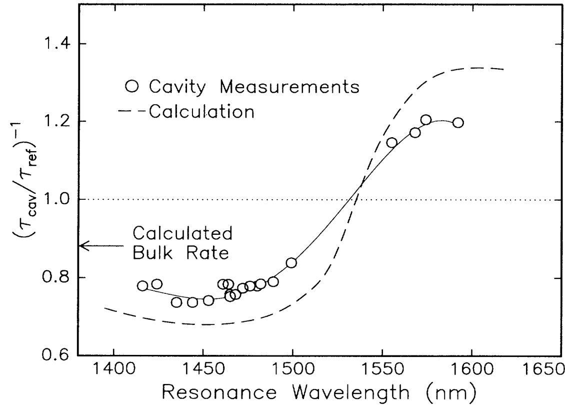

FIG. 3. The spontaneous emission rates (inverse emission lifetimes) of cavities with various resonance wavelengths, as referenced to a cavity without top mirror. Each cavity had a different thickness central SiO_2 region, altering the on-axis resonance wavelength. The calculated rate of emission in bulk SiO_2 is also shown.

reaches a maximum at ~1590 nm (with a corresponding τ_{cav} of 9.1 ms), where the entire emission peak is enhanced.

It is now useful to compare these data to calculated values of altered emission rates inside a cavity. Total emission rate calculation methods have been proposed previously for emitting media surrounded by perfect metallic reflectors [14], or equal reflectivity mirrors [12], or for certain other nonabsorbing structures [10,15]. Our method, however, is general to any low-absorption structure, and includes the possibility of waveguiding modes. The basis of the method is to calculate the electric field, $\mathbf{E}$, at the position of a dipole in the cavity with polarization $\hat{\boldsymbol{\mu}}$, after normalizing the field over a length much larger than the cavity. The emission rate then follows from the integration of the product $(\hat{\boldsymbol{\mu}}\cdot\mathbf{E})^2$ over all optical modes and dipole orientations.

Consider a planar structure consisting of $(s-2)$ thin layers surrounded by thick dielectric cladding layers numbered 1 and s. For a particular mode j, the electric field in each layer f consists of a forward- and backward-going wave with complex amplitudes $C_{j,f}$ and $D_{j,f}$ at angle θ_f from the normal. The z-direction (see inset in Fig. 1) dependence of the wave amplitudes can be calculated for any particular set of boundary conditions by employing a matrix formalism [16]. The index of refraction in layer f is given by n_f. The electric field for mode j at a position z in layer f at time t is given by

$$\mathbf{E}_{j,f}(\mathbf{r})=[C_{j,f}e^{ik_{j,f}z}\hat{\mathbf{u}}+D_{j,f}e^{-ik_{j,f}z}\hat{\mathbf{v}}]e^{i(\beta_j x-\omega t)}.$$

If k_0 is the magnitude of the free space wave vector, then β_j is the magnitude of the wave vector in the direction parallel to the layer planes. The value $k_{j,f}$ is the amplitude of the wave vector perpendicular to the layers in material f and is given by $k_{j,f}=[n_f^2k_0^2-\beta_j^2]^{1/2}$, where the argument of the bracketed term is defined to be between $-\pi/2$ and $3\pi/2$. The direction vectors $\hat{\mathbf{u}}$ and $\hat{\mathbf{v}}$ are along the y axis for TE-polarized modes, and in the x-z plane for TM-polarized modes (also known as S and P modes). The bracketed expression defines for each layer the z dependence of the electric field for mode j, and is denoted by $\mathbf{U}_j(z)$.

The total spontaneous emission rate of an emitting atom in a bulk material of index n_a is given by A_a. The radiative emission rate for an atom at position z_a out of a planar structure consisting of s layers is given by

$$A_{\mathrm{rad}}=A_a\sum_{j=1}^{4}\left(\frac{1}{2}\right)\int_0^{\theta_{\mathrm{crit}}}\left[\frac{3}{2n_a}\varepsilon_0M_j^2|\hat{\boldsymbol{\mu}}\cdot\mathbf{U}_j(z_a)|^2\right]\left(\frac{H(\theta_1)+H(\theta_s)}{H(\theta_1)\cos\theta_1+H(\theta_s)\cos\theta_s}\right)n_m^2\cos\theta_m\sin\theta_m\,d\theta_m\,,$$

$$M_j^2=\frac{L_z}{\int_{\text{all layers}}\varepsilon(z)|\mathbf{U}_j(z)|^2dz}=\frac{2}{\varepsilon_0[n_1H(\theta_1)(|C_{j,1}|^2+|D_{j,1}|^2)+n_sH(\theta_s)(|C_{j,s}|^2+|D_{j,s}|^2)]}\,.$$

The variable $H(\theta)$ is equal to 1 for real values of θ, and 0 otherwise. For a random dipole polarization $\hat{\boldsymbol{\mu}}$, $|\hat{\boldsymbol{\mu}}\cdot\mathbf{U}_j(z_a)|^2$ averages to $|\mathbf{U}_j(z_a)|^2/3$. The summation j is over the two polarization modes TE and TM, and over the two orthogonal solutions for any one angle and polarization. We define the layer m as the layer containing the atom, but it could be any layer providing the correct integration limits are used. The integration angle limit $\theta_m=\theta_{\mathrm{crit}}$ is the angle at which total internal reflection occurs between layer m and the cladding layer with the largest index, or $\pi/2$, whichever occurs first. The value M_j is a normalization constant, calculated assuming that the thickness of layers 1 and s are defined as $L_z/2n_1$ and $L_z/2n_s$, where L_z is an arbitrarily large value. If θ_1 or θ_s is nonreal, then there is only one mode solution for each polarization, with boundary conditions $C_{j,1}=0$ or $D_{j,s}=0$, respectively. If both θ_1 and θ_s are real, then two solutions exist for each polarization mode. These can be found by setting $D_{j,s}=0$ in the first calculation to yield the mode $\mathbf{U}_j$, and $C_{p,s}=0$ in the second to give solution $\mathbf{V}_p$ (not the final mode). The second mode $\mathbf{U}_q$ is generated to be orthogonal [12] to $\mathbf{U}_j$ by setting $\mathbf{U}_q=b\mathbf{U}_j+\mathbf{V}_p$, where b is a complex number with the following value:

$$b=-\frac{C_{j,1}^*C_{p,1}+D_{j,1}^*D_{p,1}}{|C_{j,1}|^2+|D_{j,1}|^2+(n_s/n_1)|C_{j,s}|^2}\,.$$

In our structure we integrate the radiative emission from the cavity over the angular range θ_m from 0 to $\pi/2$ assuming that layer m is the SiO_2 active region containing the Er atom. Some authors [10] prefer defining layer m to be either layer 1 or layer s, whichever has the higher

index. Using our choice of layer m as being the active layer, leaky waveguiding modes in the silicon layers are missed, but their contribution to the total spontaneous emission rate can be calculated using the following formula:

$$A_{\mathrm{wav}}=A_a\sum_j \pi\frac{\mathrm{Re}(\beta_j)}{k_0^2}\mathrm{Re}\left[\frac{d\beta_j}{dk_0}\right]\left[\frac{3}{2n_a}\varepsilon_0 M_j^2|\hat{\mu}\cdot\mathbf{U}_j(z_a)|^2\right],\quad M_j^2=1\Big/\int\varepsilon(z)|\mathbf{U}_j(z)|^2dz\,.$$

The (discrete) TE-polarized and TM-polarized waveguiding modes are calculated [16] using the simultaneous boundary conditions $C_{j,1}=0$ and $D_{j,s}=0$. The derivative $d\beta_j/dk_0$ is calculated by solving for β_j with two slightly different k_0 values. The integration in M_j^2 is over all layers. For a leaky mode, the mode wave vector β_j is complex and the waves can freely propagate in one of the thick cladding layers, making the mode non-normalizable. Therefore, when calculating M_j^2, the integration is arbitrarily cut off 10 nm into the layer where the light freely propagates (the silicon substrate). The total spontaneous emission rate for a particular emission wavelength and atom position is the sum of A_{rad} and A_{wav}.

We now use this calculation method to determine the theoretical Er^{3+} lifetime changes for cavities of various λ_{res} around 1535 nm. The mirrors were designed to have maximum reflectivity at 1500 nm, regardless of active region thickness. For any particular active region thickness (with corresponding λ_{res}), the emission rates at a wavelength λ_0 for atoms in the different active region positions were averaged using the implant concentration profile. The emission rates for all λ_0 were then averaged, weighted by the natural emission spectrum of Fig. 1. This resulted in an emission rate for a particular cavity λ_{res}, normalized to the bulk rate. The experimental reference rate, however, does not reflect the bulk rate. Based on the method above, we estimate the bulk rate to be $0.88\times$(the rate in the reference structure), as indicated in Fig. 3. The final calculated rates, normalized to the reference rate, are plotted as the dashed line in Fig. 3. Fair agreement is achieved for all resonance wavelengths. At shorter wavelengths than $\sim$1535 nm, the emission rate is suppressed compared to the reference structure due to the elimination of resonant emission out the top of the structure. There is still emission, however, at high emission angles and into leaky waveguiding modes in the silicon. In comparison, the emission rate is enhanced for structures resonant at a wavelength longer than $\sim$1535 nm because of the resonant emission that exists at some small angle from the normal. The maximum observed emission rate enhancement and suppression are smaller than in theory, possibly due to a nonideal mirror structure and perhaps to some nonradiative decay. Note that there is little significant lifetime change for structures resonant at the Er emission maximum of 1535 nm. This is a result of the fact that the emission rate is enhanced for shorter emission wavelengths, and suppressed for longer emission wavelengths in roughly the same amount.

In conclusion, we have realized transparent Er-doped ($\lambda/2$) Si/SiO_2 microcavities and have studied the modified Er^{3+} spontaneous emission characteristics. By changing the cavity thickness, the on-axis resonance wavelength was tuned to either side of the 1535 nm spectral maximum of the erbium emission. The effect of the cavity on the spontaneous lifetime showed a clear trend of lifetime enhancement (up to $\tau_{\mathrm{cav}}=14.8$ ms) for resonance wavelengths shorter than the Er^{3+} peak at $\sim$1535 nm, and lifetime reduction (down to $\tau_{\mathrm{cav}}=9.1$ ms) for resonance wavelengths longer than $\sim$1535 nm. Because photon reabsorption is negligible and the emission is from atomic states, the spontaneous emission rates could, for the first time, be compared successfully to a general model of emission rates of active media in dielectric microcavities.

We gratefully acknowledge P. C. Becker for assistance with the PL measurements and for stimulating discussions.

[1] E. M. Purcell, Phys. Rev. **69**, 681 (1946).
[2] P. Goy, J. M. Raimond, M. Gross, and S. Haroche, Phys. Rev. Lett. **50**, 1903 (1983).
[3] F. DeMartini, G. Innocenti, G. R. Jacobivitz, and P. Mataloni, Phys. Rev. Lett. **59**, 2995 (1987).
[4] M. Suzuki, H. Yokoyama, S. D. Brorson, and E. P. Ippen, Appl. Phys. Lett. **58**, 998 (1991).
[5] H. Yokoyama, K. Nishi, T. Anan, H. Yamada, S. D. Brorson, and E. P. Ippen, Appl. Phys. Lett. **57**, 2814 (1990).
[6] E. Yablonovitch, T. J. Gmitter, and R. Bhat, Phys. Rev. Lett. **61**, 2546 (1988).
[7] W. J. Miniscalco, J. Lightwave Technol. **9**, 234 (1991).
[8] E. F. Schubert, A. M. Vredenberg, N. E. J. Hunt, Y.-H. Wong, P. C. Becker, J. M. Poate, D. C. Jacobson, L. C. Feldman, and G. J. Zydzik, Appl. Phys. Lett. **61**, 1381 (1992).
[9] A. Polman, D. C. Jacobson, D. J. Eaglesham, R. C. Kistler, and J. M. Poate, J. Appl. Phys. **70**, 3778 (1992).
[10] G. Björk, S. Machida, Y. Yamamoto, K. Igeta, Phys. Rev. A **44**, 669 (1991).
[11] N. E. J. Hunt, E. F. Schubert, R. A. Logan, and G. J. Zydzik, Appl. Phys. Lett. **61**, 2287 (1992).
[12] K. Ujihara, Jpn. J. Appl. Phys. **30**, L901 (1991).
[13] A. M. Vredenberg, N. E. J. Hunt, E. F. Schubert, P. C. Becker, D. C. Jacobson, J. M. Poate, and G. J. Zydzik, Nucl. Instrum. Methods Phys. Res. (to be published).
[14] S. D. Brorson, H. Yokoyama, and E. P. Ippen, IEEE J. Quantum Electron. **26**, 1492 (1990).
[15] D. G. Deppe and C. Lei, J. Appl. Phys. **70**, 3443 (1991).
[16] L. M. Walpita, J. Opt. Soc. Am. A **2**, 595 (1985).